NASA Technical Memorandum

NASA TM - 103590

R-19

A GENERALIZED REUSABLE GUIDANCE ALGORITHM FOR OPTIMAL AEROBRAKING

By G.A. Dukeman

Systems Analysis and Integration Laboratory
Science and Engineering Directorate

July 1992

National Aeronautics and Space Administration

George C. Marshall Space Flight Center

TABLE OF CONTENTS

LIST OF ILLUSTRATIONS

LIST OF TABLES

TECHNICAL MEMORANDUM

A GENERALIZED REUSABLE GUIDANCE ALGORITHM FOR OPTIMAL AEROBRAKING

I. INTRODUCTION

The use of planetary atmospheres for aerobraking as a means of saving propellant has been discussed and studied extensively since the first paper on the subject appeared in 1961.[1] Many studies have concluded that significant propellant savings can be realized[2–5] compared with all-propulsive orbit transfer. The amount of savings depends on the mission scenario and the weight of the thermal protection system (TPS) required to protect the spacecraft from the aerodynamic heating incurred during the deepest penetration of the atmosphere. Reference 6 is an excellent survey of aerobraking studies.

In the past, aerobraking guidance algorithms[7] have been developed with computational efficiency as one of the major design goals, an obvious carryover from an earlier period when computing capability was a mere fraction of what it is today. Thus, simplifying assumptions were made in order to avoid numerical integration of the equations of motion. As a result, the guidance algorithms were not very general or adaptable for future aerobraking mission planning. The speed of today's computers permits more realistic, and therefore more general, real-time guidance modeling. A big advantage in this approach is the reduction in premission analyses required to determine appropriate values for mission-dependent parameters that are needed because of the simplifying assumptions. For example, the guidance algorithm for the aeroassist flight experiment (AFE)[8] used the following guidance law for determining commanded bank angle:

$$\cos(\phi_{cmd}) = \cos(\phi_{eq}) + K_q\left(K_{q_{ref}}\frac{m\left(\frac{V^2}{r}-g\right)-1}{C_L Sq}\right) + \frac{K_{\dot{r}}}{q}(\dot{r}-\dot{r}_{ref}) \quad , \tag{1}$$

where ϕ_{eq} is the bank angle required to maintain "equilibrium flight," K_q is a premission determined gain on dynamic pressure, $K_{q_{ref}}$ is a premission determined gain to provide guidance margin, and $K_{\dot{r}}$ is a premission determined gain on altitude rate error (actual minus commanded). The gain, $K_{\dot{r}}$, has two empirically derived values, one for the entry phase (also, the equilibrium glide phase) and one for the exit phase which begins when velocity magnitude has decreased to below a premission determined "trigger velocity." Yet another premission determined "transition velocity range" dictates how to smoothly transition to the exit phase. There are also premission-determined values for the plane controller logic. The form for equation (1) was presumably derived on a highly empirical basis as are the gain values and some of the other mission-dependent parameters. The algorithm to be described in this report represents a more direct "mapping" from the real-world problem of successfully aerobraking into the aerobraking guidance domain where that problem is solved. The result, it is believed, is an algorithm that is less empirical and easier to use and understand.

The next section will serve to introduce guidance concepts by discussing a simple apoapsis controller. Section III will discuss an optimal real-time apoapsis controller and the optimization results on which it is based. In section IV, a newly developed orbital plane controller will be discussed. Numerical testing and results are discussed and presented in sections V and VI. Finally, conclusions are made in section VII.

II. BASIC REAL-TIME APOAPSIS CONTROLLER

The strategy here is to numerically simulate, within the guidance, one or more planar aerobraking trajectories flown at constant bank angle. Based on the results of the simulated trajectories, the constant bank angle required to attain the target apoapsis radius at atmospheric exit can be determined. The following set of planar equations of motion,[9] for example, may be used for computing integrated trajectories:

$$dr/dt = v \sin \gamma$$

$$dv/dt = -D_a - g \sin \gamma$$

$$d\gamma/dt = L_a \cos \phi / v + (v/r - g/v) \cos \gamma \ , \tag{2}$$

where r is vehicle position magnitude, v is inertial velocity magnitude, γ is the inertial flight path angle, D_a is the aerodynamic drag acceleration, L_a is the lift acceleration, and g is the gravitational acceleration. Estimated density as a function of altitude is needed in the integration process and can be computed from a simple onboard exponential model combined with a density estimator. Density, ρ_{est}, is estimated each guidance cycle from navigation measurements

$$\rho_{est} = 2\, m D_{meas} / (S C_D V_r^2) \ , \tag{3}$$

where D_{meas} is the measured acceleration component in the relative velocity direction. From this, a multiplier, k_{rho} is computed

$$k_{rho} = \rho_{est} / \rho_{\text{model}}(h) \ , \tag{4}$$

and, thus for the current guidance cycle, the entire density profile can be estimated as

$$\rho(h) = k_{rho}\, \rho_{\text{model}}(h) \ , \tag{5}$$

the assumption being that the relative difference between the model density and encountered density is constant or at least slowly varying. In practice, to reduce the effect of noise, the k_{rho} used in equation (5) is actually the output of a low-pass filter driven by the k_{rho} in equation (4). Note that accurate calculation of D_a and L_a in equation (2) requires knowledge of relative velocity magnitude which is not obtainable from equation (2). Past experience shows that we can generally assume that the difference between inertial and relative velocity magnitudes is a constant throughout the trajectory. Alternatively, more generality could be gained by using a sixth-order differential system for the cost of additional complexity and computation. In any case, the problem of determining the appropriate bank angle, ϕ, is mathematically that of determining the zero of the nonlinear function

$$\psi(\phi)|_{r=rex} = r_{at} - r_a(r, v, \gamma)|_{r=rex} \ , \tag{6}$$

where r_{at} is the target radius of apoapsis, and r_a is the radius of apoapsis, a function of the simulated vehicle state, r, v, γ. The initial conditions are derived from the onboard navigation system. There are a number of techniques available to solve equation (6) including Newton's method or variants thereof. In practice, one Newton update (of required bank angle) is all that is required per guidance cycle, meaning either one trial trajectory plus one variational trajectory (in the case of the variational form[10] of

Newton's method) or two trial trajectories (in the case of finite difference form of Newton's method) must be generated per guidance cycle. (Actually, it is even possible to solve equation (3) using only one integrated trajectory per guidance cycle and information from the integrated trajectory from the previous guidance cycle.) The advantage of the variational form is that finite difference error does not affect the accuracy of the Jacobian used in the Newton update, whereas a disadvantage of the variational form is that anytime a change is made in the differential equation model, the variational equations have to be changed also—a tedious task. The disadvantage of the finite difference form is that robust logic has to be developed to generate accurate Jacobians, and that two separate trajectories have to be generated per guidance cycle. The advantage is that once the logic has been developed, it is valid for any guidance model changes that may be deemed necessary.

To improve numerical conditioning, the solution of equation (3) is actually obtained by iterating on the cosine of ϕ instead of ϕ directly. If the solution for a given guidance cycle happens to result in $|\cos(\phi)| > 1$ (this is referred to as guidance saturation), then one simply limits the bank command to 0° or 180° as appropriate. For the next guidance cycle, one uses the solution from the previous guidance cycle as the initial guess even if $|\cos(\phi)| > 1$. This is perfectly acceptable in computing integrated trajectories because, by inspection of equation (2), $\cos(\phi)$ is just a scalar multiplying the lift acceleration.

A. Variational Equations

A set of variational equations used to solve equation (6) is developed here. The Newton iteration for cosine of bank, $c\phi$, can be written

$$c\phi_{i+1} = c\phi_i - \frac{\psi}{d\psi/d(c\phi)} , \tag{7}$$

where ψ is the constraint function on apoapsis, and $d\psi/d(c\phi)$ is the sensitivity or Jacobian, both of which are evaluated at atmospheric exit. Using conservation of energy and angular momentum, the constraint function can be expressed as

$$\psi = \psi(r,v,\gamma) = 1+2\mu(1/r_{at}-1/r)/v^2-r^2\cos^2\gamma/r_{at}^2. \tag{8}$$

The Jacobian, $d\psi/d(c\phi)$, is expressed as

$$\frac{d\psi}{d(c\phi)} = \frac{\partial\psi}{\partial r}\frac{\partial r}{\partial\gamma}\frac{d\gamma}{d(c\phi)} + \frac{\partial\psi}{\partial v}\frac{\partial v}{\partial\gamma}\frac{d\gamma}{d(c\phi)} + \frac{\partial\psi}{d\gamma}\frac{d\gamma}{d(c\phi)} . \tag{9}$$

It is a routine matter to obtain the partials of ψ with respect to r, v, and γ. To obtain the rest of the components of the Jacobian, we make use of the relation

$$d(\partial x(t)/\partial\alpha)/dt = \partial(dx(t)/dt)/\partial\alpha = \partial(f(x(t)))/\partial\alpha , \tag{10}$$

where $dx/dt = f(x(t))$. According to equation (10), the time derivative of the sensitivity of $x(t)$ to some α is simply the partial of dx/dt with respect to α. Using this gives the following variational equations

$$d(\partial r/\partial\gamma)/dt = \partial(dr/dt)/\partial\gamma = \partial(v \sin\gamma)/\partial\gamma = \partial v/\partial\gamma \sin\gamma + v\cos\gamma \ ,$$

$$d(\partial v/\partial\gamma)/dt = -D_a(d\rho/dh\ \partial r/\partial\gamma/\rho + 2\ \partial v/\partial\gamma/V_r) + 2g\ \partial r/\partial\gamma \sin\gamma/r - g\cos\gamma \ , \qquad (11)$$

$$d(\partial\gamma/\partial c\phi)/dt = L_d/v \ ,$$

with the initial conditions

$$\partial r/\partial\gamma(t = t_0) = 0$$

$$\partial v/\partial\gamma(t = t_0) = 0 \qquad (12)$$

$$\partial\gamma/\partial c\phi\,(t = t_0) = 0 \ .$$

Thus, we can obtain, via numerical integration, the partials, $\partial r/\partial\gamma$, $\partial v/\partial\gamma$, and $\partial\gamma/\partial(c\phi)$, at any given time. In practice, we simultaneously propagate the states, r, v, γ, and the partials $\partial r/\partial\gamma$, $\partial\gamma/\partial\gamma$, and $\partial\gamma/\partial c\phi$, to atmospheric exit resulting in all the information needed in the Newton iteration equation (7). Though it is not strictly correct to propagate the state and the partials simultaneously (the equations are to be evaluated along the nominal trajectory, equation (10)), doing so is a reasonable approximation and provides for efficient computation. The formulation and implementation of the variational equations can be numerically verified by comparing the Jacobian computed using finite differences and the Jacobian computed using the variational formulation.

B. Numerical Integration

Many efficient numerical integrators exist today. The adaptive step size fifth-order Runge-Kutta-Fehlberg numerical integrator was chosen because it is accurate, efficient, and requires a relatively small amount of code and overhead. The integrated trajectories do not need to be computed very accurately because navigation errors and modeling errors cause loss of trajectory accuracy anyway. Experience has shown that 0.1 km in position error in the integration is adequate. Typically, no more than 15 to 20 integration steps are required to compute an integrated trajectory.

C. "Trappedness" Indicator

To ensure that the integration process inside the guidance is robust, a test must be implemented to detect simulated vehicles that are "trapped" in the atmosphere due to too much negative lift being modeled. It is desirable to detect trapped guidance model vehicles as early in the integration as possible to avoid wasting computation time since trapped trajectories yield no useful information except for possibly providing a lower (or upper) bound on required bank angle. Also, for the sake of robustness, the test must always detect trapped trajectories, and must never provide a false indication of "trappedness." The following condition has been found to be a useful indicator of trappedness

$$\gamma < 0 \quad \text{and} \quad d\gamma/dt < 0 \ . \qquad (13)$$

III. OPTIMAL REAL-TIME APOAPSIS CONTROLLER

Extensive aerobraking trajectory optimization work has been done in recent years.[3 11–19] The basis for the strategy used here is suggested by the results of optimization work done by Miele and others.[20] The following is an interpretation of two important results from that work:

1. Given atmospheric entry velocity and flight path angle, the optimal trajectory is a 2-arc trajectory; an entry arc flown at full positive lift, and an exit arc flown at full negative lift.

2. Given atmospheric entry velocity only, the optimal trajectory is a 1-arc trajectory flown at full negative lift.

Here, optimal is used in the sense of minimum peak heating rate, minimum structural loading, and minimum fuel usage for post-aeropass orbit insertion. Strictly speaking, the peak heating rate and structural loading are not mathematically minimized. However, optimization results have shown that the optimal trajectories discussed here are characterized by relatively small values of peak heating rate and structural loading. The optimal trajectories are constrained by equation (6), the apoapsis constraint, at aeropass exit. Note that result 2 can be thought of as a special case of result 1 where the switch to full negative lift occurs at entry.

Numerical generation of optimal trajectories in a nonreal-time environment is simple (once the form is known) in that in the case of result 1, all that is needed is to iterate on a switching time (i.e., the time to switch from full positive lift to full negative lift) such that the vehicle attains the target radius of apoapsis at aeropass exit. In the case of result 2, all that is needed is to determine the shallowest flight path angle such that at full negative lift, the vehicle attains the target radius of apoapsis at aeropass exit.

In a real-time guidance environment, result 2 does not have much practical use since the concern is with the trajectory from atmospheric entry to exit, and the entry flight path angle obviously cannot be influenced once at entry. Rather, result 2 is suggestive of a premission or preentry optimization (to determine entry flight path) that must be done in conjunction with a real-time guidance algorithm based on result 1. Thus, the guidance strategy discussed here is derived with result 1 as a starting point.

Result 1 cannot be used directly because the magnitude of dispersions (atmospheric, commanded bank angle reversals, navigation errors, etc.) that would be encountered during the exit (negative lift) phase is unknown. If result 1 is used directly and, for example, the encountered atmospheric density is less than the atmospheric model predicted, there would not be enough lift capability to prevent a premature "skipout." What is needed is some margin for uncertainties that the vehicle will encounter during the exit phase. This margin can be obtained by "tricking" the guidance into "thinking" the vehicle's full negative-lift capability is less than what it really is. This is done by introducing a "bank margin," a premission determined positive number, which is used during the entry phase modeling of the exit (i.e., negative lift) arc. This has the effect of causing the guidance logic to "think" it needs to start the exit phase earlier than it really needs to. Once the exit phase has been triggered, we simply solve for the bank angle required to hit the target apoapsis.

It turns out that there is no need to rigorously "solve" for the switching time. All that is required is to generate one integrated trajectory per guidance cycle (during the entry phase) and monitor the results. The following algorithm is used as the entry phase guidance logic:

1. Given the current vehicle state and estimates for vehicle characteristics, numerically integrate the chosen equations of motion from t_0 to $t_0+\Delta t_{roll}$ using full lift up. Here, Δt_{roll} is the estimated time duration required for the vehicle to roll from full positive lift to full negative lift.

2. Given the simulated vehicle state from step 1, numerically integrate from $t_0+\Delta t_{roll}$, using a bank angle corresponding to full negative lift less the bank margin, until the simulated vehicle either becomes trapped in the atmosphere or exits the atmosphere.

3. If the simulated vehicle becomes trapped in the atmosphere, then command the bank angle corresponding to full positive lift for the vehicle, i.e., when

$$\mathrm{sgn}(C_L) = 1 \ , \quad \phi_{cmd} = 0 \ ,$$

when

$$\mathrm{sgn}(C_L) = -1 \ , \quad \phi_{cmd} = 180 \ . \tag{14}$$

4. If the simulated vehicle exits the atmosphere, then compute the radius of apoapsis. If the radius of apoapsis is smaller than the target radius of apoapsis, then command a full positive lift bank angle. If the radius of apoapsis is larger than the target, then the exit phase is initiated, and exit phase logic will be executed on subsequent guidance cycles.

For the exit phase logic, simply use the basic apoapsis controller discussed above.

A most pleasing feature to note here is that all of the gains and many of the mission-dependent parameters so common in other guidance algorithms have been replaced by a single mission-dependent parameter, i.e., the bank margin in step 2. Another elegant feature is that the time to transition from entry to exit phase is determined completely in real time and autonomously (no trigger or transition velocities are necessary). A computationally desirable feature is that in the entry phase, only one integrated trajectory need be generated and, furthermore, early in the aeropass these are short-lived trajectories as simulated vehicles become trapped in the atmosphere. The exit phase, which is inherently more computationally intensive, does not start until the time-to-exit has been reduced somewhat in the entry phase.

IV. REAL-TIME ORBITAL PLANE CONTROLLER

The form of the plane controller is based on a first-order system where the state variable being controlled is the out-of-plane velocity component, that is, the vehicle's velocity component along a unit vector perpendicular to the desired orbit plane. The only time this quantity is zero (during any finite time period) is when the vehicle's orbit plane is identically the desired orbit plane. Thus, if the magnitude of out-of-plane velocity is driven to a small value, the same should automatically be accomplished with the plane error. Starting with the homogeneous equation:

$$dy/dt + y/t = 0 \ , \tag{15}$$

where y is the current out-of-plane velocity (measured positive along the unit vector antiparallel to the desired unit angular momentum vector), one assumes the out-of-plane lift component is the only significant out-of-plane force to obtain

$$L_a \sin \phi + \dot{y}/t = 0 \ . \tag{16}$$

Solving for sin ϕ and expanding L_a one obtains

$$\sin \phi = (y) / \tau \rho_{est} V_r^2 C_L S/(2\ \mathrm{m}) \ , \tag{17}$$

where ρ_{est} is the estimated density at the current altitude. The sign of sin ϕ gives the appropriate sign of the bank command, and the magnitude of sin ϕ is a measure of the current plane error. The following defines the plane controller logic:

When the magnitude of sin ϕ is larger than some positive number S_{max}, set the sign of the commanded bank angle to that of sin ϕ

$$\mathrm{sgn}(\phi_{cmd}) = \mathrm{sgn}(\sin \phi) \ . \tag{18}$$

This commanded bank sign will be used in subsequent guidance cycles until sin ϕ changes sign again and $|\sin \phi|$ becomes larger than S_{max}. Inspection of equation (17) reveals that the magnitude of sin ϕ becomes larger as dynamic pressure decreases. This results in increased sensitivity to plane error as atmospheric exit is approached and less sensitivity to plane error when dynamic pressure is large. This is precisely what is desired because large plane errors deep in the atmosphere are acceptable, i.e, there is plenty of controllability available during the ascent to atmospheric exit to correct for large plane errors. Note that the time constant, τ, and S_{max} are not independent parameters, but rather a doubling in τ, for example, results in the same performance as does a doubling in S_{max}. Therefore, S_{max} is arbitrarily set to one, and satisfactory guidance performance is achieved by adjusting τ. Thus, as in the apoapsis controller case, the fortuitous situation occurs wherein only one critical parameter value needs to be (semi-)rigorously determined prior to a mission. An important point is that large values of τ result in fewer roll reversals and large plane error at exit, while conversely, small values of τ result in more roll reversals and small plane error at exit. Thus, it is a simple matter to tradeoff roll reversals for plane error to obtain satisfactory performance.

V. NUMERICAL TESTING

A version of the guidance logic discussed above has been coded into a FORTRAN subroutine, GREGOAER, in as general a manner as possible to enable use with different planets, vehicles, and entry conditions. A three degree-of-freedom (DOF) aerobraking guidance algorithm test-bed program was used to test both GREGOAER and a version of what was to be flown as AFE guidance. The test mission is essentially the AFE mission (geosynchronous Earth orbit (GEO) to low-Earth orbit (LEO) transfer with $L/D \approx 0.3$) with a nominal vehicle mass of 1,860 kg, nominal entry speed of 10,308 m/s, and nominal entry flight path angle of –4.45°. No additional effort was made to optimize the AFE guidance performance over and above what was done during its extensive development. Likewise, no effort was made to optimize the guidance performance of GREGOAER, except for the newly developed lateral guidance logic. A 45° bank margin was chosen for exit arc modeling in the GREGOAER entry phase. This choice was completely arbitrary. Vehicle mass dispersions (±13.6 kg, 1σ), entry flight path dispersions (±0.01°, 1σ) and atmospheric dispersions (generated using the GRAM atmosphere[21]) were modeled for 100 test trajectories.

VI. NUMERICAL RESULTS

Time histories of several important variables are shown in figures 1 through 7 for the nominal aeropass trajectory guided by GREGOAER. The high-frequency components seen in the relative velocity, heat rate, and dynamic pressure plots are due to the perturbing winds generated by GRAM. The test-bed program provides a realistic modeling of the finite response time required for the actual bank angle to track the commanded bank angle. This is seen in the bank angle plot, figure 6. To avoid losing

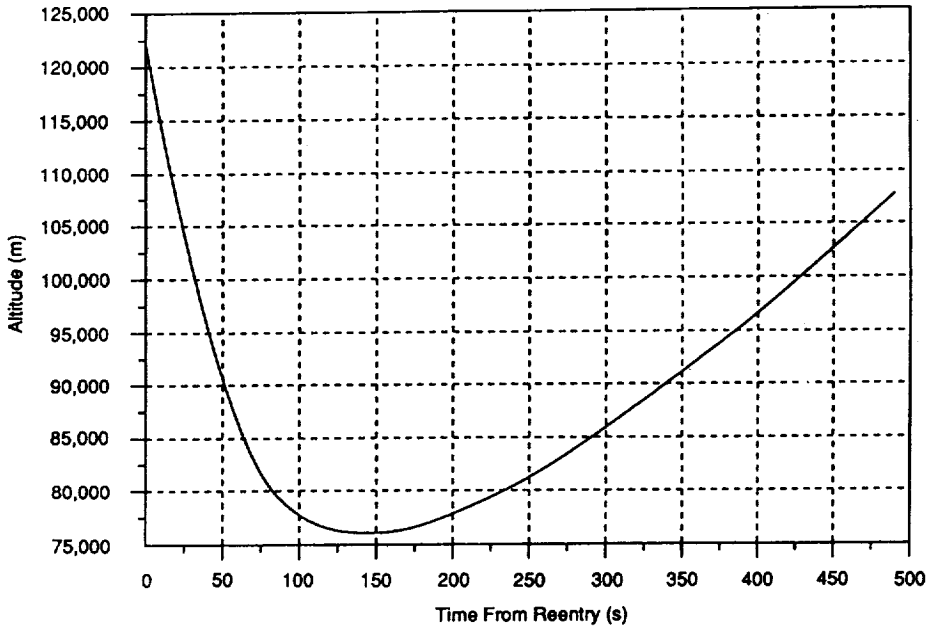

Figure 1. Nominal trajectory: altitude versus time.

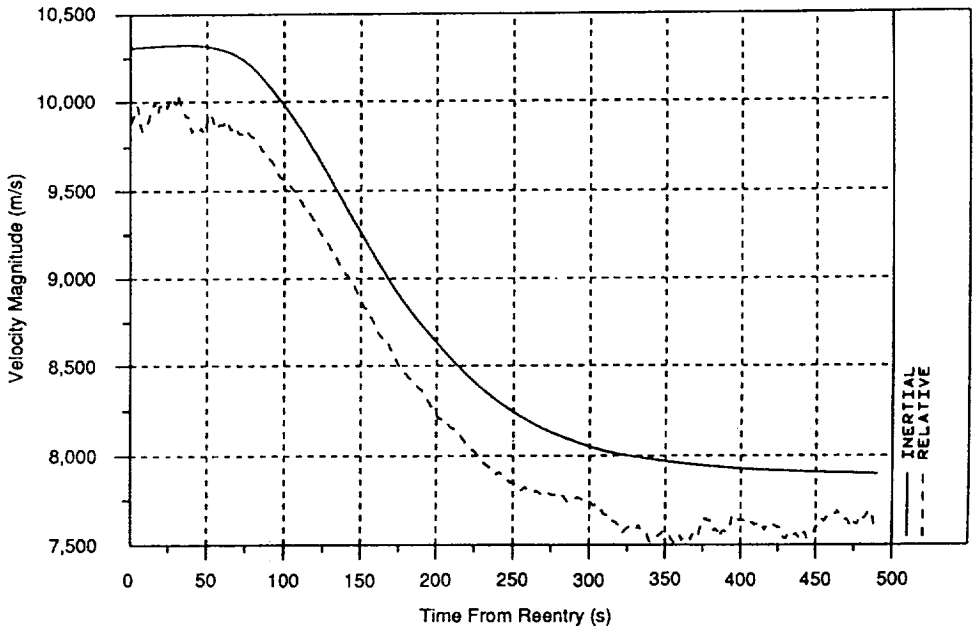

Figure 2. Nominal trajectory: inertial velocity magnitude versus time.

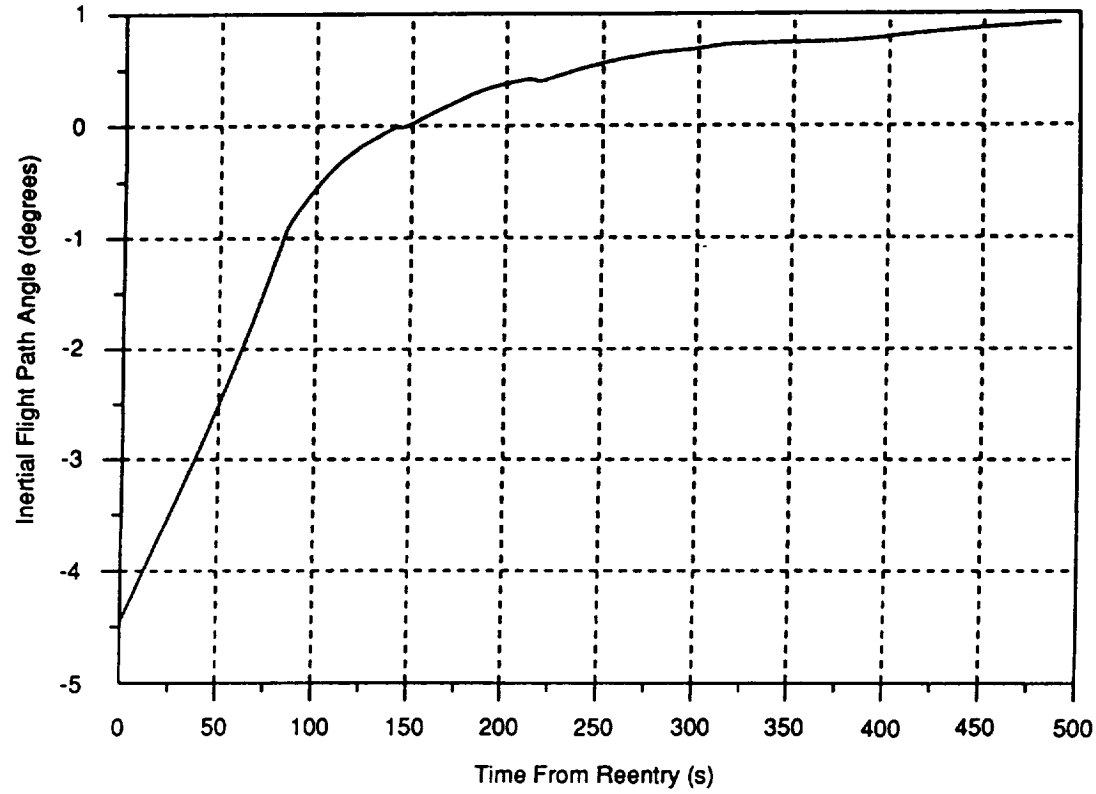

Figure 3. Nominal trajectory: inertial flight path angle versus time.

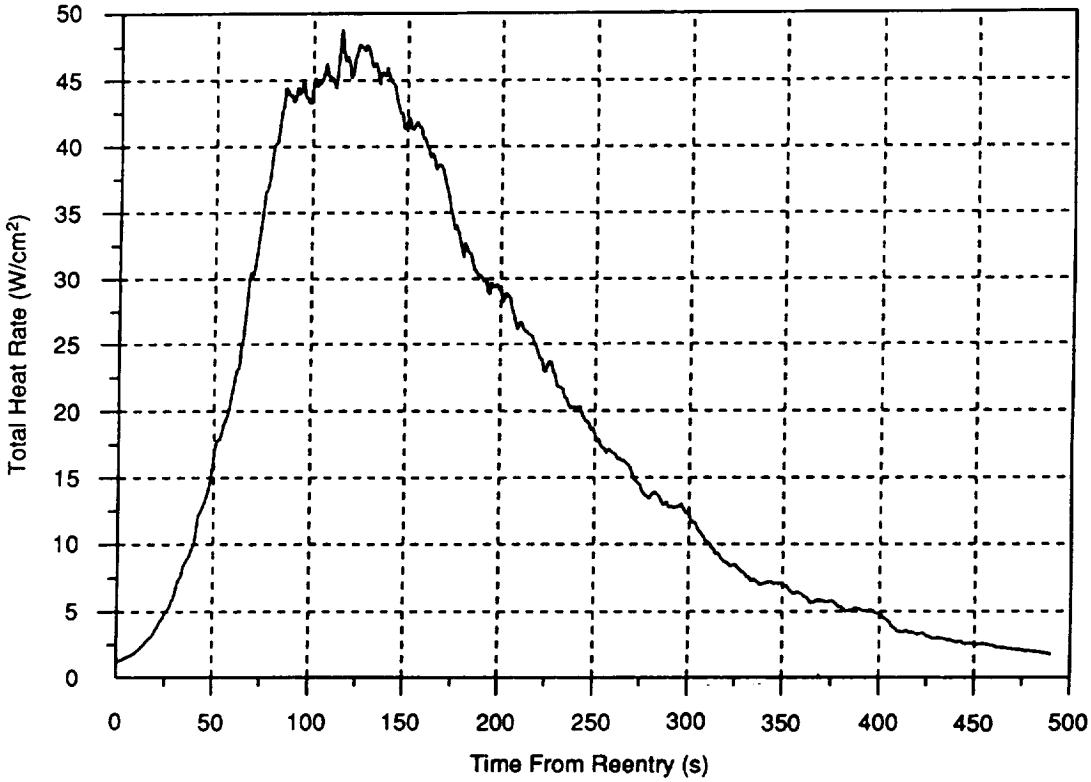

Figure 4. Nominal trajectory: total heat rate versus time.

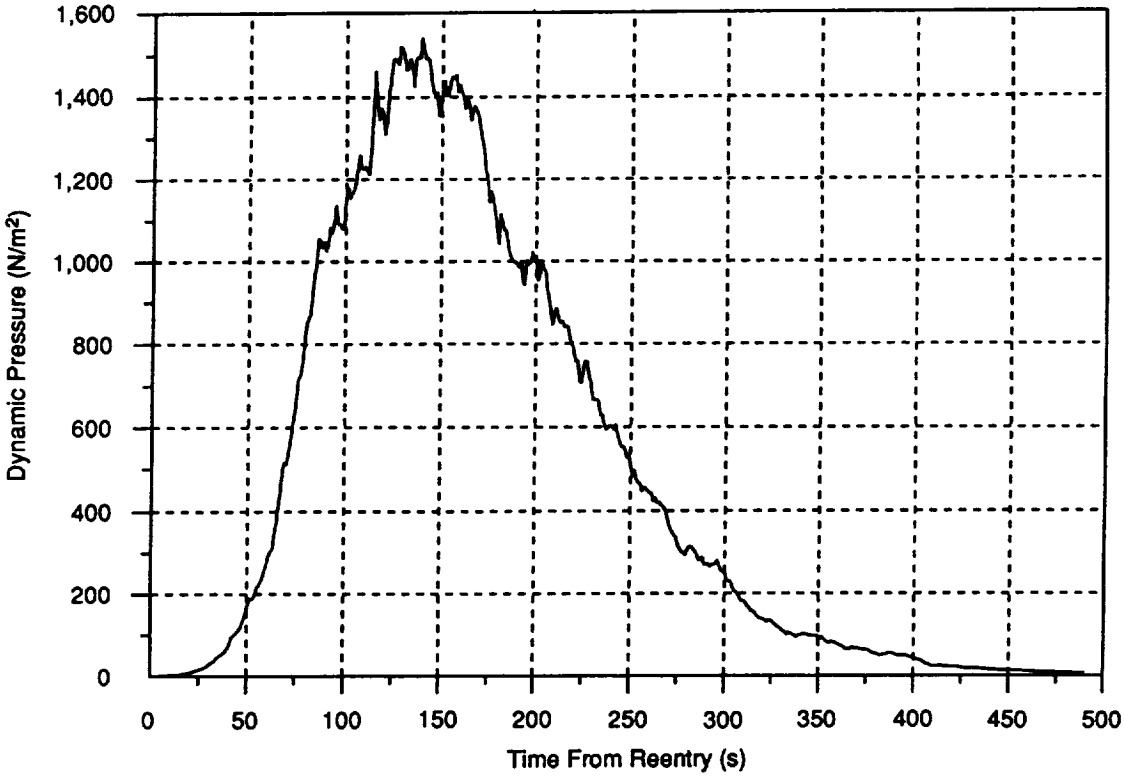

Figure 5. Nominal trajectory: dynamic pressure versus time.

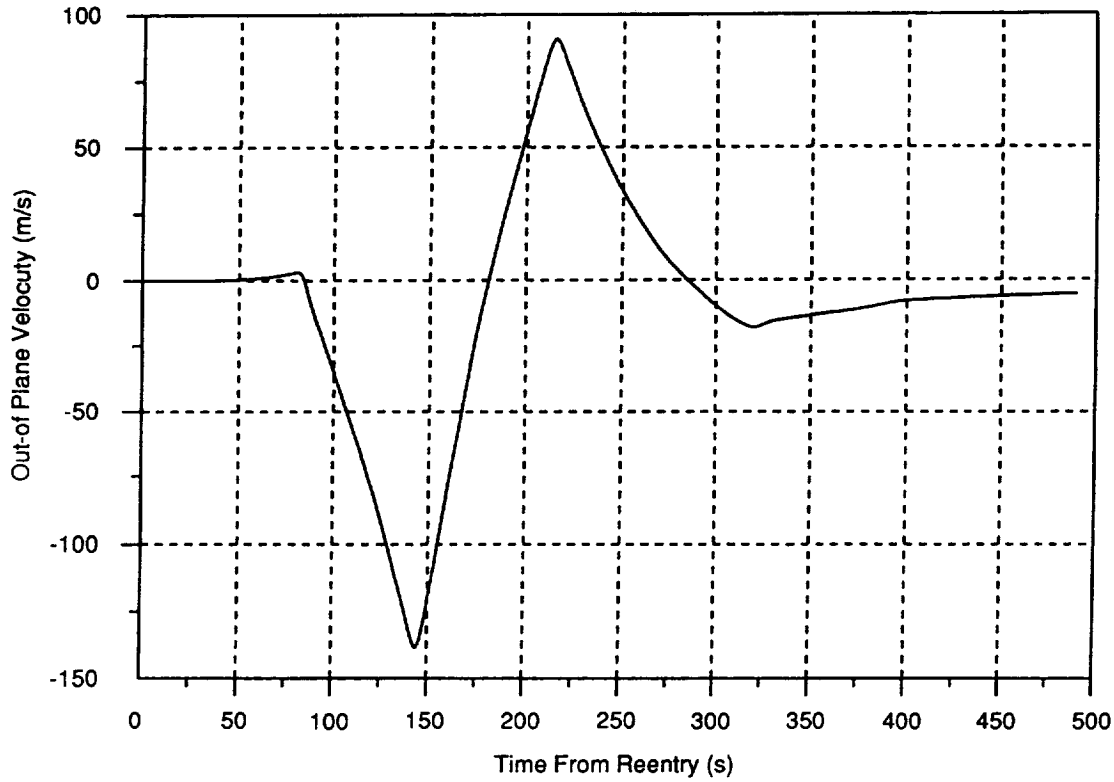

Figure 6. Nominal trajectory: out-of-plane velocity component versus time.

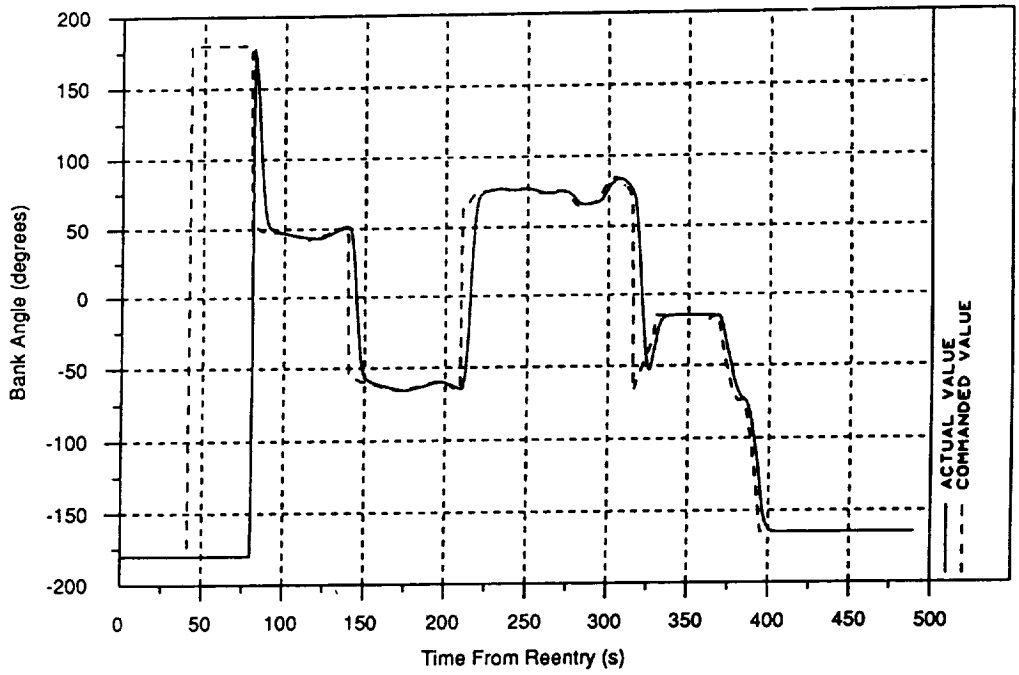

Figure 7. Nominal trajectory: bank angle versus time.

plane controllability, the commanded bank angle magnitude is limited between 15° and 165°. This limiting typically occurs in the latter part of the exit phase and is seen in figure 6 after about 325 s into the aeropass. By limiting the bank angle, only about 3 percent of inplane lift capability is sacrificed, while a relatively large out-of-plane lift component (0.26 L_a) is provided. Roll reversals at about 145, 210, and 310 s are seen in the bank angle plot. The effect of these is seen in figure 7. As demonstrated in the out-of-plane velocity plot, the plane controller becomes more sensitive (more likely to command a roll reversal) to plane error as dynamic pressure, hence controllability, decreases.

Statistics of important trajectory characteristics for the 100 trajectories using the AFE guidance are given in table 1, while the results using GREGOAER are given in table 2.

Table 1. Results using AFE guidance algorithm.

	Mean	Min	Max
Minimum altitude, m	75,138	74,368	75,808
Peak G-load, g	2.04	1.85	2.25
Peak dyn pr, N/m^2	1,800	1,652	2,025
Peak ht rt, W/cm^2	51.0	47.6	54.1
Heat load, J/cm^2	8,152	7,768	8,472
Exit apogee, km	328.0	289.3	344.1
Exit perigee, km	12.8	−11.7	42.0
Exit wedge, degree (°)	9.76E−2	7.23D−2	0.14
Delta V, m/s	106.8	97.5	118.3
Roll Reversals	2.8	2	4

Table 2. Results using GREGOAER guidance algorithm.

	Mean	Min	Max
Minimum altitude, m	76,133	75,066	77,178
Peak G-load, g	1.80	1.57	2.09
Peak dyn pr, N/m^2	1,594	1,379	1,853
Peak ht rt, W/cm^2	49.6	46.0	53.1
Heat load, J/cm^2	8,816	8,382	9,380
Exit apogee, km	342.2	319.0	359.4
Exit perigee, km	52.9	25.8	77.4
Exit wedge, degree (°)	3.7E–2	1.1E–2	6.4E–2
Delta V, m/s	90.1	80.7	98.8
Roll Reversals	3.9	3	5

Note that the minimum altitudes experienced using GREGOAER are higher than those of AFE guidance resulting in lower loads and lower peak heat rates. GREGOAER total heat loads are higher because the times spent in the atmosphere are typically higher (by about 100 s). Neither AFE guidance nor GREGOAER had any problem hitting the target apogee of 340 km, although GREGOAER had a smaller spread between the maximum and minimum values which is a desirable feature. GREGOAER had higher exit perigees resulting in smaller post-aeropass delta V. GREGOAER did a better job minimizing the exit wedge angle (angle between the desired and actual planes), at a cost of one more roll reversal on average. A plane controller value of $\tau = 45$ s was used here. The average and worst-case circularization (at 296 km) delta-V requirements for GREGOAER are significantly smaller due mainly to the higher exit perigees.

VII. CONCLUSIONS

With a bare minimum of development effort, the guidance algorithm discussed here is producing desirable results. Because it was based on sound physical principles and on optimality results, there is reason to believe it can provide superior and robust guidance performance for a wide variety of aerobraking missions with a minimum of laborious and costly premission guidance performance analyses. Current and future work in the area of onboard density profile estimators would also significantly improve guidance performance by reducing the bank margin required in the entry phase logic.

REFERENCES

1. London, H.S.: "Change of Satellite Orbit Plane by Aerodynamic Maneuvering." Journal of the Aerospace Sciences, March 1962, pp. 323–332.

2. Mulqueen, J., and Coughlin, D.: "Lunar Mission Aerobrake Performance Study." NASA TM-103562, December 1991.

3. Hanson, J.M.: "Combining Space-Based Propulsive Maneuvers and Aerodynamic Maneuvers to Achieve Optimal Orbital Transfer." Journal of Guidance, Control, and Dynamics, vol. 12, No. 5, September–October 1989, pp. 732–738.

4. National Aeronautics and Space Administration: "Report of the 90-Day Study on Human Exploration of the Moon and Mars." November 1989.

5. French, J.R., and Cruz, M.I.: "Aerobraking and Aerocapture for Planetary Missions." Astronautics and Aeronautics, February 1980.

6. Walberg, G.D.: "A Survey of Aeroassisted Orbit Transfer." Journal of Spacecraft and Rockets, vol. 2, No. 1, January–February 1985, pp. 3–18.

7. Gamble, J.D., Cerimele, C.J., Moore, T.E., and Higgins, J.: "Atmospheric Guidance Concepts for an Aeroassist Flight Experiment." The Journal of the Astronautical Sciences, vol. 36, Nos. 1/2, January–June 1988, pp. 45–71.

8. "Aeroassist Flight Experiment—Guidance and Navigation System Design Book." MDC 91W5016, McDonnell Douglas Space Systems Company, June 1991.

9. Vinh, N.X.: "Optimal Trajectories in Atmospheric Flight." Elsevier Scientific Publishing Company, New York, 1981.

10. Kirk, D.E.: "Optimal Control Theory." Prentice-Hall Inc., Englewood Cliffs, New Jersey, 1970, pp. 343–357.

11. Mease, K.D., and Vinh, N.X.: "Minimum-Fuel Aeroassisted Coplanar Orbit Transfer Using Lift-Modulation." Journal of Guidance, Control, and Dynamics, vol. 8, January–February 1985, pp. 134–141.

12. Vinh, N.X., Johannesen, J.R., and Hanson, J.M.: "Explicit Guidance of Drag-Modulated Aeroassisted Transfer Between Elliptical Orbits." Journal of Guidance, Control, and Dynamics, vol. 9, May–June 1986, pp. 274–280.

13. Hull, D.G., Giltner, J.M., Speyer, J.L., and Mapar, J.: "Minimum Energy-Loss Guidance for Aeroassisted Orbital Plane Change." Journal of Guidance, Control, and Dynamics, vol. 8, July–August 1985, pp. 487–493.

14. Hull, D.G., and Speyer, J.L.: "Optimal Reentry and Plane-Change Trajectories." The Journal of the Astronautical Sciences, vol. XXX, No. 2, April–June 1982, pp. 117–130.

15. Frostic, F., and Vinh, N.X.: "Optimal Aerodynamic Control by Matched Asymptotic Expansions." Acta Astronautica, vol. 3, pp. 319–332.

16. Miele, A., Basapur, V.K., and Mese, K.D.: "Nearly-Grazing Optimal Trajectories for Aeroassisted Orbital Transfer." The Journal of the Astronautical Sciences, vol. 34, No. 1, January–March 1986, pp. 3–18.

17. Miele, V.K., Basapur, V.K., and Lee, W.Y.: "Optimal Trajectories for Aeroassisted, Noncoplanar Orbital Transfer." Acta Astronautica, vol. 15, No. 6/7, 1987, pp. 399–411.

18. Miele, A., and Basapur, V.K.: "Approximate Solutions to Minimax Optimal Control Problems for Aeroassisted Orbital Transfer." Acta Astronautica, vol. 12, No. 10, 1985, pp. 809–818.

19. Miele, A., and Venkataraman, P.: "Optimal Trajectories for Aeroassisted Orbital Transfer." Acta Astronautica, vol. 11, No. 7–8, 1984, pp. 423–433.

20. Miele, A.: "Progress in the Optimization and Guidance of Trajectories for AOT and AFE Vehicles." Presentation to NASA-MSFC, July 1990.

21. Justus, C.G.: "The NASA/MSFC Global Reference Atmospheric Model—MOD 3." NASA Contractor Report 3256, 1980.

22. Chapra, S.C., and Canale, R.P.: "Numerical Methods for Engineers." Second edition, McGraw-Hill Book Company, New York, 1988, p. 617.

APPROVAL

A GENERALIZED RESUABLE GUIDANCE ALGORITHM FOR OPTIMAL AEROBRAKING

By G.A. Dukeman

The information in this report has been reviewed for technical content. Review of any information concerning Department of Defense or nuclear energy activities or programs has been made by the MSFC Security Classification Officer. This report, in its entirety, has been determined to be unclassified.

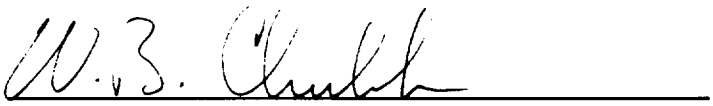

W.B. CHUBB
Director, Systems Analysis and Integration Laboratory

☆ U.S. GOVERNMENT PRINTING OFFICE 1992–631-060/60145

REPORT DOCUMENTATION PAGE

Form Approved
OMB No. 0704-0188

1. AGENCY USE ONLY *(Leave blank)*	2. REPORT DATE	3. REPORT TYPE AND DATES COVERED
	July 1992	Technical Memorandum

4. TITLE AND SUBTITLE

A Generalized Reusable Guidance Algorithm for Optimal Aerobraking

5. FUNDING NUMBERS

6. AUTHOR(S)

G.A. Dukeman

7. PERFORMING ORGANIZATION NAME(S) AND ADDRESS(ES)

George C. Marshall Space Flight Center
Marshall Space Flight Center, Alabama 35812

8. PERFORMING ORGANIZATION REPORT NUMBER

9. SPONSORING/MONITORING AGENCY NAME(S) AND ADDRESS(ES)

National Aeronautics and Space Administration
Washington, DC 20546

10. SPONSORING/MONITORING AGENCY REPORT NUMBER

NASA TM - 103590

11. SUPPLEMENTARY NOTES

Prepared by Systems Analysis and Integration Laboratory, Science and Engineering Directorate.

12a. DISTRIBUTION/AVAILABILITY STATEMENT

Unclassified—Unlimited

12b. DISTRIBUTION CODE

13. ABSTRACT *(Maximum 200 words)*

A practical real-time guidance algorithm has been developed for guiding aerobraking vehicles in such a way that the maximum heating rate, the maximum structural loads, and the post-aeropass delta-V requirement (for post-aeropass orbit insertion) are all minimized. The algorithm is general and reusable in the sense that a minimum of assumptions are made, thus minimizing the number of gains and mission-dependent parameters that must be laboriously determined prior to a particular mission. A particularly interesting feature is that inplane guidance performance is tuned by simply adjusting one mission-dependent parameter, the bank margin; similarly, the out-of-plane guidance performance is tuned by simply adjusting a plane controller time constant. Other objectives in the algorithm development are simplicity, efficiency, and ease of use. The algorithm is developed for, but not necessarily restricted to, a single pass mission and a trimmed vehicle with bank angle modulation as the method of trajectory control. Guidance performance is demonstrated via results obtained using this algorithm integrated into an aerobraking test-bed program. Comparisons are made with numerical results from a version of the aerobraking guidance algorithm that was to be flown onboard NASA's aeroassist flight experiment (AFE) vehicle. Promising results are obtained with a minimum of development effort.

14. SUBJECT TERMS

Aerobraking, Real-Time Guidance, Atmospheric Guidance, Optimal Trajectory

15. NUMBER OF PAGES

19

16. PRICE CODE

NTIS

17. SECURITY CLASSIFICATION OF REPORT	18. SECURITY CLASSIFICATION OF THIS PAGE	19. SECURITY CLASSIFICATION OF ABSTRACT	20. LIMITATION OF ABSTRACT
Unclassified	Unclassified	Unclassified	Unlimited